crystallization papers

Purification, crystallization and preliminary X-ray diffraction of a complex between IL-10 and soluble IL-10R1

Kristopher Josephson,[a,b] David T. McPherson[c] and Mark R. Walter[a,b]*

[a]Center for Biophysical Sciences and Engineering, University of Alabama at Birmingham, Birmingham, AL 35294, USA, [b]Department of Microbiology, University of Alabama at Birmingham, Birmingham, AL 35294, USA, and [c]Center for Aids Research, University of Alabama at Birmingham, Birmingham, AL 35294, USA

Correspondence e-mail: walter@uab.edu

A complex between interleukin-10 and the extracellular domain of its high-affinity receptor (sIL-10R1) has been crystallized from polyethylene glycol solutions. Crystals suitable for diffraction analysis required the modification of the NXS/T glycosylation sites on sIL-10R1 by site-directed mutagenesis and inclusion of the detergent cyclohexyl-methyl-β-D-maltopyranoside in the crystallization experiments. The crystals belong to space group $P3_212$ or its enantimorph $P3_112$, with unit-cell parameters $a = b = 46.23$, $c = 307.78$ Å, $\alpha = \beta = 90$, $\gamma = 120°$, and diffract X-rays to ~2.9 Å. The IL-10 dimer is positioned on a crystallographic twofold, resulting in one IL-10 chain and one sIL-10R1 chain in the asymmetric unit, which corresponds to a solvent content of approximately 44%.

1. Introduction

Interleukin-10 (IL-10) is a pleiotropic cytokine with broad anti-inflammatory effects that include down-regulating the expression of several inflammatory cytokines and MHC class II presentation (Moore *et al.*, 2001). IL-10 is also capable of promoting antibody production, proliferation and differentiation by B cells. Cellular responses to IL-10 are mediated by two cell-surface receptors IL-10R1 (Ho *et al.*, 1993; Liu *et al.*, 1994) and IL-10R2 (Kotenko *et al.*, 1997), which are members of the class II cytokine receptor family. Members of this family contain homologous extracellular cytokine-binding domains and include receptors for interferons α, β and γ, as well as the IL-10 homologues IL-20 and IL-22 (Kotenko & Pestka, 2000; Kotenko *et al.*, 2001; Xie *et al.*, 2000). IL-10 signaling is initiated by the sequential assembly of IL-10, IL-10R1 and IL-10R2 into a cell-surface complex that mediates the cytoplasmic protein–protein interactions required for its specific cellular responses.

The crystal structure of IL-10 revealed a helical homodimer, topologically equivalent to interferon-γ (IFNγ), which folds as two distinct domains oriented at ~90° to one another (Walter & Nagabhushan, 1995; Zdanov *et al.*, 1995). In solution, IL-10 and the extracellular domain of IL-10R1 (sIL-10R1) form a complex of two IL-10 dimers and four sIL-10R1 chains (Tan *et al.*, 1995). The stoichiometry of this complex differs from the 1:2 stoichiometry observed in the homologous IFNγ–sIFNγR1 crystal structure (Walter *et al.*, 1995). Currently, the role of the 2:4 IL-10–

IL-10R1 complex in signaling is unknown. In order to define the interactions that mediate its assembly, we have crystallized IL-10 in complex with sIL-10R1.

2. Materials and methods

2.1. Cloning, expression and purification

IL-10 was expressed and purified as described previously (Josephson *et al.*, 2000). Incorporation of SeMet into IL-10 (Se-IL-10) was accomplished by *Escherichia coli* expression of IL-10 in a Met auxotroph, B834 (Novagen), grown in M9 minimal media supplemented with 50 mg l^{-1} SeMet (Hendrickson *et al.*, 1990).

For sIL-10R1, a DNA fragment was amplified from the IL-10R1 cDNA (accession No. UOO672) by PCR using the 5′ primer GTATTGATATCGCCGCCACCATGCTGC-CGTGCCTCGTAGTGC and the 3′ primer ATAAGAATGCGGCCGCTCAGTTGGTC-ACGGTGAAATACTGCCTG. The PCR product was digested with *Eco*RV and *Not*I and ligated into the expression plasmid pMt/V5-HisB (Invitrogen) to generate pMt-sIL-10R1. Mutation of the six potential N-linked glycosylation sites (Asn29, Asn53, Asn89, Asn133, Asn156 and Asn158) to glutamine was accomplished using the Quick Change Mutagenesis Kit (Strategene), resulting in pMt-sIL-10R1Q6.

Transfection and selection of *Drosophila* S2 cells with either pMt-sIL-10R1 or pMt-sIL-10R1Q6 and the hygromycin resistance vector (pCoHYGRO) were performed as suggested by the manufacturer (Invitrogen). Expression

was induced at a cell density of 5×10^6 cells ml^{-1} by addition of 200 mM Cu$_2$SO$_4$ (final concentration of 0.5 mM) and was allowed to proceed for 4 d. Secreted sIL-10R1 was purified from the culture medium using an IL-10 affinity column as previously described (Tan *et al.*, 1995).

2.2. Characterization of sIL-10R1 and its glycosylation

EndoglycosidaseD (Seikagaku Corporation) and PNGaseF (New England Biolabs) were used for enzymatic deglycosylation of sIL-10R1 and the IL-10–sIL-10R1 complex respectively, under native conditions (20 mM Tris–HCl, 150 mM NaCl pH 8.0 at 277 K for 24 h). The purity and heterogeneity of sIL-10R1 was assessed by electrophoresis using 15% SDS polyacrylamide gels. N-terminal sequencing was performed on a Beckman Model PI 2090E microsequencer. Samples for MALDI-TOF mass spectrometry (MS) were analyzed on a Voyager Elite mass spectrometer (Perseptive Biosystems).

2.3. Complex purification

IL-10–receptor complexes were formed by incubating IL-10 with sIL-10R1 (or sIL-10RQ6) at a 2:1 (sIL-10R1–IL-10 dimer) molar ratio for 1 h at 277 K. Complexes were purified by gel-filtration chromatography using two Superdex-200 (10 × 300 mm) columns linked in tandem and equilibrated in 20 mM Tris–HCl, 150 mM NaCl pH 8.0 at a flow rate of 0.35 ml min^{-1}. The concentrations of the purified complexes were estimated assuming a 100% recovery of the initial IL-10 and sIL-10R1 components.

2.4. Crystallization

All crystallization experiments employed the hanging-drop method. Initial crystallization screens were performed with Crystal Screen I and Membfac kits (Hampton Research) at 296 and 277 K. The best crystals of the IL-10–sIL-10R1Q6 complex were grown by streak seeding 2 µl drops containing 5 mg ml^{-1} of the IL-10–sIL10R1Q6 complex, 10 mM Tris–HCl pH 8.0, 75 mM NaCl, 50 mM MgCl$_2$, 50 mM ADA [N-2-(acetamido)iminodiacetic acid] pH 6.2, 4% PEG 6000, 1 mM cyclohexylmethyl-β-D-maltopyranoside (Cymal-6) and equilibrated at 296 K against a well solution consisting of 0.1 M ADA pH 6.2, 8% PEG 6000 and 0.1 M MgCl$_2$. Crystals of the complex between Se-IL-10 and sIL-10R1Q6 were grown under the same conditions

following streak seeding with IL-10–sIL-10R1Q6 microseeds.

2.5. X-ray diffraction

Crystals were flash-cooled for low-temperature data collection in a nitrogen stream (100 K) following exchange of the drop solution with a solution of 10% PEG 6000, 0.1 M ADA pH 6.2, 0.1 M MgCl$_2$ and 20% PEG 400. Diffraction data were collected at SSRL beamline 9-2 equipped with a Quad 4 CCD detector. Reflection intensities were integrated and scaled using *MOSFLM* and *SCALA* (Collaborative Computational Project, Number 4, 1994).

3. Results and discussion

3.1. Characterization of *Drosophila*-expressed sIL-10R1.

Expression of sIL-10R1 in *Drosophila* S2 cells in conjunction with a single ligand-affinity step yielded 1.5 mg of sIL-10R1 per liter of culture. N-terminal sequencing identified the first six residues of the secreted sIL-10R1 as H1-G2-T3-E4-L5-P6, which is identical to sIL-10R1 produced by myeloma cells (Tan *et al.*, 1995).

SDS–PAGE analysis of sIL-10R1 revealed two major bands which migrated between the 25 and 30 kDa molecular-weight markers. MALDI-TOF MS analysis of sIL-10R1 revealed two broad peaks centered at molecular masses of 27 297 and 28 111 Da (Fig. 1a). Previous characterization of insect-cell glycosylation has shown the most common N-linked glycan to be a hexasaccharide of 1039 Da (Manneberg *et al.*, 1994). The predicted molecular weight of sIL-10R1 is 24 392 Da. Therefore, mass analysis suggests the majority of sIL-10R1 expressed in this system has three (predicted mass, 27 509 Da) or four (predicted mass, 28 548 Da) of the six potential N-linked glycosylation sites (NXS/T) occupied. A minor band is also observed by SDS–PAGE that migrates slightly slower than the two major bands and is likely to correspond to a sIL-10R1 species with five of the six NXS/T sites utilized.

As previously described, enzymatic removal of sIL-10R1 glycosylation with PNGaseF resulted in the precipitation of the receptor even at relatively dilute concentrations (Hoover *et al.*, 1999). However, precipitant was not observed upon treatment of the IL-10–sIL-10R1 complex with excess amounts of PNGaseF; this resulted in a single sIL-10R1 species with molecular mass of ~25 kDa as analyzed by SDS–PAGE. MALDI-TOF MS analysis of this

product indicated improved homogeneity, with two major peaks of 26 483 and 26 691 Da (Fig. 1b). These species differ by 208 Da (possibly a matrix adduct) and are ~2 kDa greater than the predicted molecular weight of sIL-10R1, indicating that the glycan moieties at two of the NXS/T sites are resistant to release by PNGaseF.

PNGaseF breaks the glycosidic bond and converts the linked Asn substrate to an Asp. Owing to the incomplete deglycosylation and solubility problems of PNGaseF-treated sIL-10R1, we also treated sIL-10R1 with EndoglycosidaseD (EndoD). EndoD breaks the chitobiose core leaving an N-acetyl-glucosamine residue (GlcNAc, 203 Da), and when present a 1–6 fucose residue (GlcNAc + fucose, 350 Da). EndoD-treated sIL-10R1 had improved solubility and did not require IL-10 to remain in solution. Mass-spectrometry analysis of this product revealed a broad peak centered at 25 746 Da, which corresponds to 'complete' deglycosylation
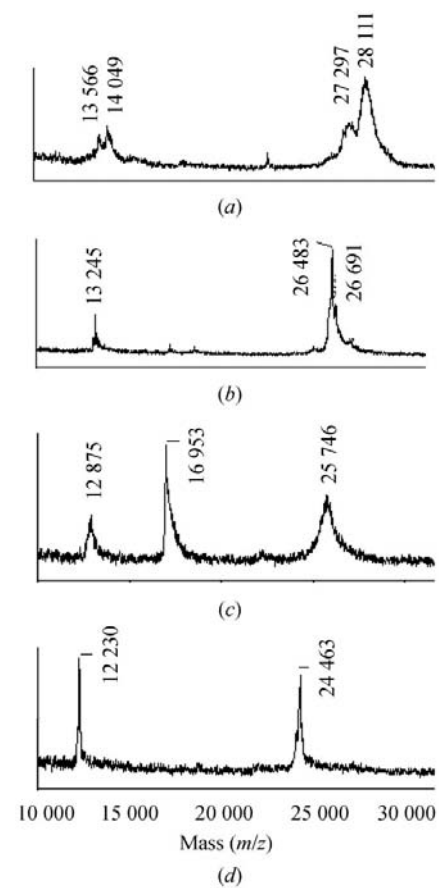

Figure 1
MALDI-TOF MS analysis of various forms of sIL-10R1. (a) Wild-type untreated sIL-10R1. (b) Wild-type sIL-10R1 treated with PNGaseF. (c) Wild-type sIL-10R1 treated with EndoglycosidaseD. The internal standard apomyoglobin is observed with an M/Z of 16 953. (d) sIL-10R1Q6. The M/Z values of ~12 000 correspond to doubly charged ($Z = 2$) sIL-10R1 species.

by EndoD (predicted mass 25 001–25 792 Da; Fig. 1c).

sIL-10R1Q6 was observed as the sharpest peak by MALDI-TOF MS with a molecular weight of 24 463 Da (predicted mass 24 462 Da; Fig. 1d). Though sIL-10R1Q6 behaved similarly to sIL-10R1 during purification and concentration, its expression was reduced relative to sIL-10R1, with a yield of 0.6 mg per liter of culture.

3.2. Complex analysis and stoichiometry

The complexes formed between IL-10 and the four forms of its receptor, sIL-10R1, PNGaseF-treated sIL-10R1, EndoD-treated sIL-10R1 and sIL-10R1Q6, were indistinguishable by gel-filtration chromatography and eluted with an apparent molecular weight of 135 kDa. However, the molecular weight of the PNGAseF-treated complex as determined by equilibrium

(a)

(b)

0.1 mm

(c)

Figure 2
Crystals of the IL-10–sIL-10R1Q6 complex. (a) Crystalline aggregate that appeared 1 d after streak seeding in the absence of the non-ionic detergent Cymal-6. (b) Crystals that appeared 3 d after streak seeding with seeds from Fig. 1(a) when 1 m*M* Cymal-6 was included. (c) Drop containing Cymal-6 with a single crystal obtained 4 d after streak seeding with seeds from Fig. 1(b).

analytical ultracentrifugation is 164 kDa, which agrees well with the expected weight (181 kDa) for a 2 IL-10: 4 sIL-10R1 complex (K. Josephson & M. R. Walter, unpublished results).

3.3. Crystallization

Crystallization trials with complex containing the fully glycosylated form of sIL-10R1 as well as complex treated with PNGaseF were unsuccessful. Microcrystals of EndoD-treated sIL-10R1 in complex with IL-10 were obtained in drops 6 and 36 of the 296 K Crystal Screen I, but could not be optimized. Crystallization trials of the complex containing sIL-10R1Q6 yielded an amorphous aggregate in drop 25 of the 296 K Membfac screen, corresponding to a well solution of 0.1 *M* ADA pH 6.5, 12% PEG 6000 and 0.1 *M* MgCl$_2$. Disruption of this aggregate with a needle resulted in a shower of tiny (5 µm) inter-grown crystals 1 d later.

Systematic screening of buffer pH, polyethylene glycols and different ions did not improve crystal size or morphology. Streak seeding improved the growth of these crystals but resulted in poorly formed crystalline aggregates (Fig. 2a). However, repeated streak seeding into drops containing Cymal-6 produced sharp single crystals (0.1–0.2 mm) in 3–4 d (Figs. 2b and 2c).

3.4. X-ray diffraction

The diffraction quality of the IL-10–sIL-10R1Q6 crystals upon exposure to synchrotron radiation was highly variable (d_{max} = 8.0–2.9 Å) and required the screening of over 100 crystals. Efforts to correlate growth and freezing conditions or crystal size and morphology with diffraction quality were unsuccessful. A complete native data set revealed the crystals belong to space group $P3_212$ or $P3_112$ (unit-cell parameters $a = b = 46.23$, $c = 307.78$ Å, $\alpha = \beta = 90$, $\gamma = 120°$; Table 1). Isomorphous crystals of the complex between SeMet-IL-10 and sIL-10R1Q6 that diffract to 3.0 Å have also been identified. Packing analysis indicates that the asymmetric unit contains one chain of IL-10 and one chain of sIL-10R1, which corresponds to a solvent content of 44% (V_M = 2.23 Å^3 Da^{-1}; Matthews, 1968). This suggests that the twofold axis of the IL-10 dimer sits on the crystallographic twofold axis of this space group.

Previously, triclinic crystals of a complex between IL-10 and enzymatically deglycosylated sIL-10R1 were grown from conditions similar to ours (12% PEG 6000, 0.1 *M*

Table 1
Data collection.

Values in parentheses are for the highest resolution shell

Wavelength (Å)	0.9184
Resolution (Å)	50–2.9 (2.97–2.90)
No. observations	24449
No. unique	8189
Redundancy	2.8 (2.4)
Completeness (%)	92.8 (75.0)
$I/\sigma(I)$	9.1 (5.2)
R_{merge} (%)	0.050 (0.122)
Unit-cell parameters	
a, b (Å)	46.23
c (Å)	307.78

† $R_{merge} = \sum |I_{hkl} - \langle I \rangle| / \sum I_{hkl}$, where the average intensity $\langle I \rangle$ is taken over all symmetry-equivalent measurements and I_{hkl} is the measured intensity for any given reflection.

sodium citrate pH 5.6, 0.1 *M* Li$_2$SO$_4$) yet only diffract X-rays to 4.5 Å (Hoover *et al.*, 1999). The higher diffraction limit of our crystals is likely to be a consequence of the increased chemical homogeneity of sIL-10R1Q6 relative to enzymatically deglycosylated sIL-10R1 and of the inclusion of Cymal-6 in the crystallization solution. The quality of our native data suggests it will be possible to determine the structure of the 2IL-10–4sIL-10R1 complex and reveal the protein–protein interactions that initiate this important biological pathway.

References

Collaborative Computational Project, Number 4 (1994). *Acta Cryst.* D**50**, 760–763.
Hendrickson, W. A., Horton, J. R. & LeMaster, D. M. (1990). *EMBO J.* **9**, 1665–1672.
Ho, A. S. Y., Liu, Y., Khan, T. A., Hse, D.-H., Bazan, J. F. & Moore, K. W. (1993). *Proc. Natl Acad. Sci. USA*, **90**, 11267–11271.
Hoover, D. M., Schalk-Hibi, C., Chou, C.-C., Menon, S., Wlodawer, A. & Zdanov, A. (1999). *Eur. J. Biochem.* **262**, 134–141.
Josephson, K., DiGiacomo, R., Indelicato, S. R., Iyo, A. H., Nagabhushan, T. L., Parker, M. H. & Walter, M. R. (2000). *J. Biol. Chem.* **275**, 13552–13557.
Kotenko, S. V., Izotova, L. S., Mirochnitchenko, O. V., Esterova, E., Dickensheets, H., Donnelly, R. P. & Pestka, S. (2001). *J. Biol. Chem.* **276**, 2725–2732.
Kotenko, S. V., Krause, C. D., Izotova, L. S., Pollack, B. P., Wu, W. & Pestka, S. (1997). *EMBO J.* **16**, 5894–5903.
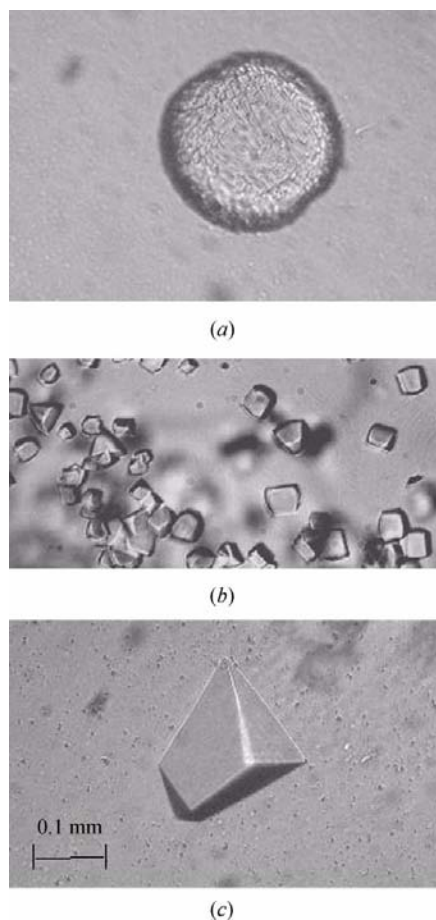Kotenko, S. V. & Pestka, S. (2000). *Oncogene*, **19**, 2557–2565.

crystallization papers

Liu, Y., Wei, S. H.-Y., Ho, A. S.-Y., de Waal Malefyt, R. & Moore, K. W. (1994). *J. Immunol.* **152**, 1821–1929.

Manneberg, M., Friedlein, A., Kurth, H., Lahm, H. & Fountouloakis, M. (1994). *Protein Sci.* **3**, 30–38.

Matthews, B. W. (1968). *J. Mol. Biol.* **33**, 491–497.

Moore, K. W., de Waal Malefyt, R., Coffman, R. L. & O'Garra, A. (2001). *Annu. Rev. Immunol.* **19**, 683–765.

Tan, J. C., Braun, S., Rong, H., DiGiacomo, R., Dolphin, E., Baldwin, S., Narula, S. K., Zavodny, P. J. & Chou, C.-C. (1995). *J. Biol. Chem.* **270**, 12906–12911.

Walter, M. R. & Nagabhushan, T. L. (1995). *Biochemistry*, **34**, 12118–12125.

Walter, M. R., Windsor, W. T., Nagabhushan, T. L., Lundell, D. J., Lunn, C. A., Zavodny, P. J. & Narula, S. K. (1995). *Nature (London)*, **376**, 230–235.

Xie, M. H., Aggarwal, S., Ho, W. H., Foster, J., Zhang, Z., Stinson, J., Wood, W. I., Goddard, A. D. & Gurney, A. L. (2000). *J. Biol. Chem.* **275**, 31335–31339.

Zdanov, A., Schalk-Hihi, C., Gustchina, A., Tsang, M., Weatherbee, J. & Wlodawer, A. (1995). *Structure*, **3**, 591–601.